diversity

MDPI

Article

The Characterization and Phylogenetic Implications of the Mitochondrial Genomes of *Antheminia varicornis* and *Carpocoris purpureipennis* (Hemiptera: Pentatomidae)

Ying Wang, Ruijuan Yang, Xiuxiu Zhu, Chenguang Zheng * and Wenjun Bu *

Institute of Entomology, College of Life Sciences, Nankai University, 94 Weijin Road, Tianjin 300071, China; 15376155087@163.com (Y.W.); yrj1523@163.com (R.Y.); xiuxiuz@163.com (X.Z.)
* Correspondence: chenguangzheng@nankai.edu.cn (C.Z.); wenjunbu@nankai.edu.cn (W.B.)

Abstract: The mitochondrial genome (mitogenome) has been widely used for structural comparisons and phylogenetic analyses of Hemiptera groups at different taxonomic levels. However, little is known about the mitogenomic characteristics of species from *Antheminia* and *Carpocoris*, two morphologically similar genera in the Pentatomidae family, and their phylogenetic relationships need to be further confirmed. In this study, the mitogenomes of *Antheminia varicornis* (Jakovlev, 1874) and *Carpocoris purpureipennis* (De Geer, 1773) were sequenced and analyzed. Coupled with previously published mitogenomes of Pentatomidae, we performed a phylogenetic analysis. The mitogenomes of *A. varicornis* and *C. purpureipennis* are conserved in terms of genomic structure, base composition, codon usage, and tRNA secondary structure. Each mitogenome contains the typical 37 genes and a control region and all genes are arranged in the same order as in the ancestral insect mitogenome. Nucleotide composition is highly biased with the third codon in PCGs displaying the highest A + T content. Phylogenetic analysis strongly supports the sister relationship between *A. varicornis* and *C. purpureipennis*. The phylogenetic trees show a strong support for the monophyly of Asopinae and Phyllocephalinae, while the monophyly of Pentatominae and Podopinae was rejected. Our study enriches the mitochondrial genome database of the genera *Antheminia* and *Carpocoris* and provides a valuable resource for further phylogenetic and evolutionary analyses of the Pentatomidae.

Keywords: *Antheminia varicornis*; *Carpocoris purpureipennis*; mitochondrial genome; phylogeny

Citation: Wang, Y.; Yang, R.; Zhu, X.; Zheng, C.; Bu, W. The Characterization and Phylogenetic Implications of the Mitochondrial Genomes of *Antheminia varicornis* and *Carpocoris purpureipennis* (Hemiptera: Pentatomidae). *Diversity* **2023**, *15*, 1209. https://doi.org/10.3390/d15121209

Academic Editor: Luc Legal

Received: 16 November 2023
Revised: 6 December 2023
Accepted: 7 December 2023
Published: 9 December 2023

1. Introduction

The typical insect mitochondrial genome (mitogenome) is a double-strand circular DNA molecule ranging from 14 kb to 20 kb in size, containing 37 genes (13 protein-coding genes, 2 ribosomal RNA genes, 22 transfer RNA genes), and a control region [1–3]. Due to its small size, maternal inheritance, low sequence recombination, and fast evolutionary rates [4,5], the mitogenome is considered a powerful marker for phylogenetic and evolutionary analyses [6–11]. In addition, comparing mitochondrial gene structure and genetic composition between species can provide crucial insights into the evolution of related species [3,12,13]. Benefiting from advances in high-throughput sequencing technology, an increasing number of mitogenomes have been sequenced among the Hemiptera [14–17] and have been widely used for mitochondrial structure comparison, phylogenetic analysis at different taxonomic levels, species delimitation, population genetic structure, and biogeographic studies [7,18–29].

Pentatomidae is one of the largest and most diverse families of Heteroptera, with a wide distribution around the world [30]. Most species are phytophagous, sucking sap from the stems, leaves, or fruits of their host plants, and pose a serious threat to a wide variety of valued crops, causing significant economic losses worldwide [31,32]. Since the publication of the first complete mitogenome of a Pentatomidae species, *Nezara viridula* (GenBank accession number NC_011755) [33], the number of mitogenomes in this family

has continued to grow [20,22,34–36]. Detailed comparative analyses of the mitogenome and phylogenetic analyses have also been performed for the Pentatomidae family [37]. However, the coverage is still limited relative to the number of species, which is quite restrictive for clarifying the phylogenetic relationships of genera and species in the Pentatomidae family. *Antheminia* Mulsant and Rey, 1866, and *Carpocoris* Kolenati, 1846, are two morphologically similar genera within the Pentatomidae family; most species in both two genera are crop pests, with adults and nymphs sucking juice from inflorescences and young stems. The yellow spots will appear on the leaves after being sucked, and the inflorescence and tender ear will wither or even fade after being seriously damaged. Many species of *Antheminia* and *Carpocoris* mainly harm cash crops such as alfalfa, wheat, potato, radish, carrot, elm, and bayberry. A previous study based on small molecular fragments (1759 bp of 18S rRNA, 646 bp of 28S rRNA, 592 bp of 16S rRNA and 564 bp of COI) revealed a sister relationship between the two genera, but there is low node support [38]. Currently, little is known about the mitogenomic characteristics of the two genera. Their molecular data are yet to be supplemented. Their phylogenetic positions in the Pentatomidae family and the phylogenetic relationships between them still need to be further confirmed.

In this study, we sequenced and annotated the mitogenomes of *Antheminia varicornis* (Jakovlev, 1874) and *Carpocoris purpureipennis* (De Geer, 1773), representing the *Antheminia* and *Carpocoris* genera, respectively. We analyzed the genomic structure, base composition, codon usage, and tRNA secondary structure of the two mitogenomes. Coupled with published mitogenomes of Pentatomidae, we carried out a phylogenetic analysis to verify the phylogenetic positions of *Antheminia* and *Carpocoris* in the Pentatomidae family and their phylogenetic relationships. This study may increase our understanding of the relationships between the *Antheminia* and *Carpocoris* genera, and also verify the phylogeny and evolution of Pentatomidae.

2. Materials and Methods

2.1. Sample Collection and DNA Extraction

The specimens of *A. varicornis* and *C. purpureipennis* were collected from Horqin Right Front Banner, Neimenggu Province, China (46.46 N, 120.31 E), on 11 July 2021 and Ziwu Mountain, Shaanxi Province, China (35.87 N, 108.55 E), on 27 July 2019, respectively. Since both species consist of unprotected invertebrates, no special permits were required to collect samples from these sites. All specimens were preserved in 100% ethanol and stored at −20 °C at the Institute of Entomology at Nankai University (Tianjin, China). All specimens were identified based on their morphology. Total genomic DNA was extracted from the thoracic muscle using a Universal Genomic DNA Kit (CWBIO, Beijing, China) and stored at −80 °C until downstream analyses.

2.2. Mitogenome Sequencing, Assembly and Annotation

The whole mitochondrial genomes were sequenced using the Illumina NovaSeq 6000 platform with a 150 bp paired-end read strategy at Novogene Co., Ltd. (Beijing, China). Low-quality reads were removed using fastp [39], and then approximately 2 Gb of clean data were obtained for each sample. The clean data from the sequencing reads were assembled using mitoZ 2.4 [40] with default settings and IDBA-UD 1.1.3 [41] with minimum and maximum k values of 40 and 120 bp, respectively. Transfer RNA (tRNA) genes and their secondary structures were identified on the MITOS2 webserver (http://mitos2.bioinf.uni-leipzig.de/index.py, accessed on 3 April 2023). The typical secondary structure for tRNAs were manually drawn according to MITOS2 predictions and using Adobe Illustrator 2021. Protein-coding genes (PCGs) and ribosomal RNA (rRNA) genes were annotated through alignment with homologous regions of previously published mitogenomes of Pentatominae in GenBank. Newly sequenced mitogenomes were submitted to GenBank (accession numbers: OR074478 and OR074479).

2.3. Bioinformatic Analyses

Mitogenome maps were drawn using the Proksee Server (https://proksee.ca, accessed on 29 May 2023) [42]. The base composition, codon usage, and relative synonymous codon usage (RSCU) values of *A. varicornis* and *C. purpureipennis* were calculated in MEGA X [43]. The bias of the nucleotide composition was measured by AT-skew [(A − T)/(A + T)] and GC-skew [(G − C)/(G + C)].

2.4. Phylogenetic Analyses

Phylogenetic analyses were performed using the newly sequenced mitogenomes of *A. varicornis* and *C. purpureipennis*, together with 28 Pentatomidae mitogenomes downloaded from GenBank (Table 1). Two species of Plataspidae were selected as outgroups (Table 1).

Table 1. Taxonomic information and GenBank accession numbers of mitochondrial genomes downloaded from GenBank in this study.

Family	Subfamily	Species	Accession Number
Pentatomidae	Asopinae	*Arma custos*	MT535604
		Cazira horvathi	NC_042817
		Dinorhynchus dybowskyi	NC_037724
		Eocanthecona thomsoni	NC_042816
		Picromerus griseus	NC_036418
		Zicrona caerulea	MW847250
	Pentatominae	*Carbula sinica*	KY069964
		Catacanthus incarnatus	MF497716
		Caystrus obscurus	MF497717
		Dalpada cinctipes	MW847236
		Dolycoris baccarum	NC_020373
		Erthesina fullo	JQ743673
		Eurydema dominulus	MW847238
		Glaucias dorsalis	MW847239
		Halyomorpha halys	NC_013272
		Hippotiscus dorsalis	MW847240
		Hoplistodera incisa	MF620037
		Menida violacea	MK617948
		Neojurtina typica	MW847243
		Nezara viridula	NC_011755
		Pentatoma metallifera	MW847244
		Placosternum urus	MF497730
		Plautia fimbriata	MF497731
		Rubiconia intermedia	KP207596
	Phyllocephalinae	*Dalsira scabrata*	NC_037374
		Gonopsis affinis	NC_036745
	Podopinae	*Graphosoma rubrolineatum*	NC_033875
		Scotinophara lurida	NC_042815
Plataspidae		*Megacopta cribraria*	OP123001
		Calacta lugubris	NC_058965

The sequences of 13 PCGs and 2 rRNA genes were aligned using MAFFT 7.402 [44]. After removing the stop codon, the alignments of individual genes were then concatenated by PhyloSuite 1.2.2 [45] to generate two datasets: PCG123R (all three codon positions of the 13 PCGs and 2 rRNAs) and PCG12R (the first and second codon positions of the 13 PCGs and 2 rRNAs). The best-fit partitioning scheme and nucleotide substitution models were identified using PartitionFinder 2.0 [46] and the Bayesian Information Criterion (BIC). Phylogenetic analyses were conducted using the Bayesian inference (BI) and maximum likelihood (ML) methods based on the two datasets. BI analysis was performed using MrBayes 3.2.7a [47] with the best-fitting substitution model (Table 2). Two simultaneous

Markov chain Monte Carlo (MCMC) runs of 10,000,000 generations were conducted, and trees were sampled every 1000 generations, with the first 25% discarded as burn-in. The convergence of runs was confirmed by checking whether the deviation of split frequencies was below 0.01. ML analysis was performed using IQ-TREE 2.2.0 [48] with 1000 bootstrap replicates under the best-fitting substitution model.

Table 2. The best model for each partition of the two datasets.

Datasets	Partition Names	Best Model
PCG123R	ND3, ATP6, COI, COIII, COII, CytB;	GTR + I + G
	ND2, ND6, ATP8;	GTR + I + G
	ND1, ND4L, ND4, ND5;	GTR + I + G
	12S rRNA, 16S rRNA.	GTR + I + G
PCG12R	ND3, ATP6, COI, COIII, COII, CytB;	GTR + I + G
	ND2, ATP8, ND6, ND4, ND1, ND5, ND4L;	TVM + I + G
	12S rRNA, 16S rRNA;	GTR + I + G

3. Results and Discussion

3.1. Mitogenome Organization and Composition

The mitogenomes of *A. varicornis* and *C. purpureipennis* are 15,251 and 15,322 bp in size, respectively. Each mitogenome contains 37 typical genes (13 PCGs, 2 rRNAs, and 22 tRNAs) and a control region. Among these genes, four PCGs (ND1, ND4, ND4L, and ND5), eight tRNAs (trnC, trnF, trnH, trnL (UAG), trnP, trnQ, trnV and trnY), and two rRNAs (12S rRNA and 16S rRNA) are encoded on the minority strand (N strand), while the other 23 genes are encoded on the majority strand (J strand) (Figure 1, Tables 3 and 4). The mitogenome of *A. varicornis* has a total of 26 bp space in seven gene overlaps, ranging in length from 1 to 8 bp; the longest overlap region fell between the tRNA-Trp and tRNA-Cys genes. In addition, there were sixteen 1–25 bp gene spacer regions, with a total length of 116 bp; the longest 25 bp intergenic spacer sequences were located between ND1 and tRNA-Ser. In the *C. purpureipennis* mitogenome, gene overlaps were found at eight gene junctions and involved a total of 35 bp; the longest 8 bp overlap was located between the tRNA-Trp and tRNA-Cys genes. Intergenic spacer sequences were found at 15 gene junctions and involved a total of 98 bp, ranging in length from 1 to 21 bp; the longest 21 bp intergenic spacer sequences were located between ND1 and tRNA-Ser. The number and arrangement of genes in both mitogenomes are conserved, consistent with those of ancestral insects [49].

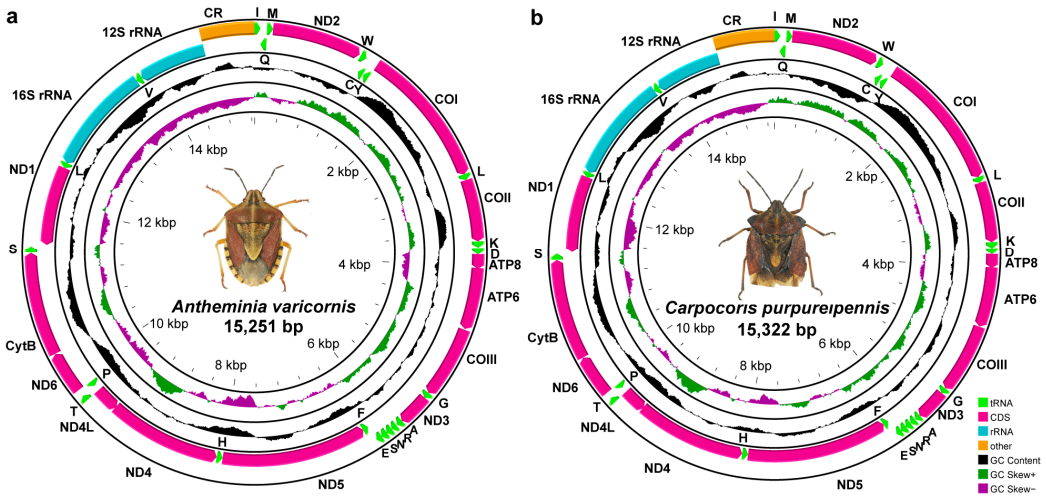

Figure 1. Mitogenome maps of *A. varicornis* (**a**) and *C. purpureipennis* (**b**). The names of PCGs and rRNAs are indicated by standard abbreviations, while names of tRNAs are represented by a single letter abbreviation.

Table 3. Organization of mitochondrial genome of *A. varicornis*.

Gene	Strand	Position		Anticodon	Size (bp)	Start Codon	Termination Codon	Intergenic Nucleotides
tRNA-I	J	1	65	GAT	65			
tRNA-Q	N	69	137	TTG	69			3
tRNA-M	J	137	202	CAT	66			−1
ND2	J	203	1186		984	ATA	TAA	0
tRNA-W	J	1204	1271	TCA	68			17
tRNA-C	N	1264	1325	GCA	62			−8
tRNA-Y	N	1335	1400	GTA	66			9
COI	J	1410	2946		1537	TTG	T-	9
tRNA-L	J	2947	3012	TAA	66			0
COII	J	3013	3691		679	ATA	T-	0
tRNA-K	J	3692	3761	CTT	70			0
tRNA-D	J	3768	3838	GTC	71			6
ATP8	J	3839	3997		159	TTG	TAA	0
ATP6	J	3991	4665		675	ATG	TAG	−7
COIII	J	4676	5464		789	ATG	TAA	10
tRNA-G	J	5467	5532	TCC	66			2
ND3	J	5533	5884		352	ATA	T-	0
tRNA-A	J	5885	5951	TGC	67			0
tRNA-R	J	5962	6025	TCG	64			10
tRNA-N	J	6027	6093	GTT	67			1
tRNA-S	J	6093	6161	GCT	69			−1
tRNA-E	J	6161	6226	TTC	66			−1
tRNA-F	N	6229	6295	GAA	67			2
ND5	N	6295	8000		1706	ATT	TA-	−1
tRNA-H	N	8002	8070	GTG	69			1
ND4	N	8072	9400		1329	ATG	TAG	1
ND4L	N	9394	9681		288	ATT	TAA	−7
tRNA-T	J	9684	9749	TGT	66			2
tRNA-P	N	9750	9815	TGG	66			0
ND6	J	9827	10,291		465	ATA	TAA	11
CytB	J	10,296	11,429		1134	ATG	TAA	4
tRNA-S	J	11,436	11,504	TGA	69			6
ND1	N	11,530	12,453		924	TTG	TAA	25
tRNA-L	N	12,454	12,518	TAG	65			0
16S rRNA	N	12,519	13,787		1269			0
tRNA-V	N	13,788	13,855	TAC	68			0
12S r RNA	N	13,856	14,656		801			0
Control Region		14,657	15,251		595			0

The nucleotide composition of the two mitogenomes is biased toward A + T, as in other Pentatomidae species [22,37]. The A + T content of the whole mitogenome is 76.7% for *A. varicornis* and 73.4% for *C. purpureipennis*. The A + T content of the protein-coding genes is 73.2% for *A. varicornis* and 72.9% for *C. purpureipennis*. The 12S rRNA and 16S rRNA exhibit a higher A + T content among the 37 typical genes in both mitogenomes. The A + T content of the third codon in PCGs is significantly higher than that of the first and second codons (Table 5). The whole mitogenome of *A. varicornis* exhibits negative AT-skew and GC-skew, while that of *C. purpureipennis* exhibits positive AT-skew and negative GC-skew. It is generally believed that asymmetric mutations at four bases and selection pressure are the two main reasons for the base composition preference of mitochondrial genome, which mainly come from the process of replication and gene transcription [50].

Table 4. Organization of mitochondrial genome of *C. purpureipennis*.

Gene	Strand	Position		Anticodon	Size (bp)	Start Codon	Termination Codon	Intergenic Nucleotides
tRNA-I	J	1	66	GAT	66			
tRNA-Q	N	64	132	TTG	69			−3
tRNA-M	J	137	202	CAT	66			4
ND2	J	203	1189		987	ATA	TAA	0
tRNA-W	J	1207	1273	TCA	67			17
tRNA-C	N	1266	1329	GCA	64			−8
tRNA-Y	N	1342	1406	GTA	65			12
COI	J	1417	2953		1537	TTG	T-	10
tRNA-L	J	2954	3019	TAA	66			0
COII	J	3020	3698		679	ATA	T-	0
tRNA-K	J	3699	3770	CTT	72			0
tRNA-D	J	3771	3838	GTC	68			0
ATP8	J	3839	3997		159	GTG	TAA	0
ATP6	J	3991	4665		675	ATG	TAA	−7
COIII	J	4671	5459		789	ATG	TAA	5
tRNA-G	J	5463	5527	TCC	65			3
ND3	J	5528	5879		352	ATA	T-	0
tRNA-A	J	5880	5942	TGC	63			0
tRNA-R	J	5948	6011	TCG	64			5
tRNA-N	J	6014	6079	GTT	66			2
tRNA-S	J	6079	6147	GCT	69			−1
tRNA-E	J	6147	6210	TTC	64			−1
tRNA-F	N	6209	6275	GAA	67			−2
ND5	N	6276	7980		1705	ATT	T-	0
tRNA-H	N	7982	8051	GTG	70			1
ND4	N	8054	9382		1329	ATG	TAA	2
ND4L	N	9376	9663		288	ATT	TAA	−7
tRNA-T	J	9666	9730	TGT	65			2
tRNA-P	N	9731	9794	TGG	64			0
ND6	J	9803	10,276		474	ATA	TAA	8
CytB	J	10,280	11,416		1137	ATG	TAA	3
tRNA-S	J	11,420	11,488	TGA	69			3
ND1	N	11,510	12,439		930	ATA	TAA	21
tRNA-L	N	12,434	12,499	TAG	66			−6
16S rRNA	N	12,500	13,771		1272			0
tRNA-V	N	13,772	13,839	TAC	68			0
12S rRNA	N	13,840	14,640		801			0
Control Region		14,641	15,322		682			0

Table 5. Nucleotide composition of mitochondrial genomes of *A. varicornis* and *C. purpureipennis*.

	Species	Whole Genome	Protein Coding Genes	1st Codon Position	2nd Codon Position	3rd Codon Position	tRNA Genes	12S rRNA	16S rRNA	Control Region
A + T %	*A. varicornis*	76.7	73.2	68.8	66.9	83.7	75.7	77.4	78.3	70.4
	C. purpureipennis	73.4	72.9	69.3	66.6	82.7	73.9	75.9	76.7	70.5
AT-Skew	*A. varicornis*	−0.14	−0.11	0.03	−0.39	−0.02	0.07	0.11	−0.13	−0.03
	C. purpureipennis	0.13	−0.11	0.03	−0.39	0.01	0.06	0.14	0.17	−0.04
GC-Skew	*A. varicornis*	−0.06	0.00	0.21	−0.10	−0.19	−0.10	−0.28	0.24	−0.24
	C. purpureipennis	−0.14	−0.01	0.21	−0.10	−0.24	−0.07	−0.25	−0.24	−0.22

3.2. Protein-Coding Genes and Codon Usage

Most PCGs of the two mitogenomes begin with the standard start codon ATN (N represents one of four nucleotides, A, T, C, or G), while COI starts with TTG. In addition, the start codons of ATP8 are TTG and GTG in *A. varicornis* and *C. purpureipennis*, respectively. The

start codon of ND1 in *A. varicornis* is TTG (Tables 3 and 4). The termination codon in nine PCGs (ATP6, ATP8, COIII, CytB, ND1, ND2, ND4, ND4L and ND6) is TAA or TAG, while COI, COII, ND3, and ND5 have incomplete termination codons (T or TA) (Tables 3 and 4) that are probably completed by post-transcriptional polyadenylation [51]. The total codon numbers (excluding the termination codons) in *A. varicornis* and *C. purpureipennis* are 3663 and 3669, respectively. The longest gene was the ND5 gene (1706 and 1705), and the shortest was the ATP8 gene (159 and 159) in *A. varicornis* and *C. purpureipennis*, respectively. The most frequently used codon families are Ile, Leu2, Met, and Phe, each numbering more than 300. The least frequently used codon family is Cys, with a total of 50 in both mitogenomes (Figure 2). The relative synonymous codon usage (RSCU) patterns for the two mitogenomes are similar, and the RSCU values are shown in Figure 3 and Table 6. For each amino acid, the most prevalently used codons are NNA and NNU (Figure 3, Table 6), which is consistent with the higher A + T content in the third codon in PCGs.

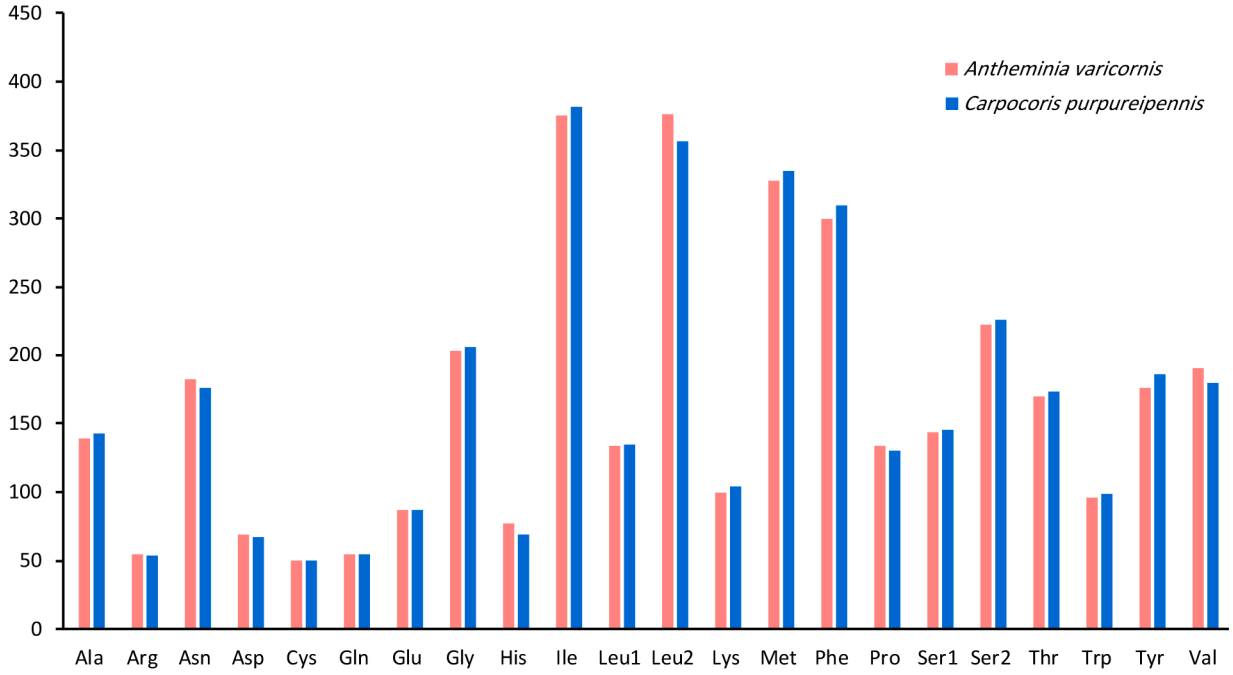

Figure 2. Patterns of codon usage in the mitogenomes of *A. varicornis* and *C. purpureipennis*. The *X*-axis shows the codon families, and the *Y*-axis shows the total codons.

Table 6. Codon and the relative synonymous codon usage (RSCU) of the mitochondrial genomes (excluding the termination codons) of *A. varicornis* and *C. purpureipennis*.

Amino Acid	Codon	*A. varicornis*		*C. purpureipennis*		Amino Acid	Codon	*A. varicornis*		*C. purpureipennis*	
		Count	RSCU	Count	RSCU			Count	RSCU	Count	RSCU
Phe	UUU(F)	243	1.62	234	1.51	Tyr	UAU(Y)	148	1.68	149	1.6
	UUC(F)	57	0.38	76	0.49		UAC(Y)	28	0.32	37	0.4
Leu	UUA(L)	335	3.94	307	3.74	His	CAU(H)	55	1.43	53	1.54
	UUG(L)	41	0.48	50	0.61		CAC(H)	22	0.57	16	0.46
	CUU(L)	52	0.61	55	0.67	Gln	CAA(Q)	44	1.6	46	1.67
	CUC(L)	5	0.06	7	0.09		CAG(Q)	11	0.4	9	0.33
	CUA(L)	65	0.76	63	0.77	Asn	AAU(N)	148	1.63	142	1.61
	CUG(L)	12	0.14	10	0.12		AAC(N)	34	0.37	34	0.39
Ile	AUU(I)	311	1.66	310	1.62	Lys	AAA(K)	76	1.52	79	1.52
	AUC(I)	64	0.34	72	0.38		AAG(K)	24	0.48	25	0.48
Met	AUA(M)	289	1.76	295	1.76	Asp	GAU(D)	55	1.59	50	1.49
	AUG(M)	39	0.24	40	0.24		GAC(D)	14	0.41	17	0.51

Table 6. *Cont.*

Amino Acid	Codon	*A. varicornis*		*C. purpureipennis*		Amino Acid	Codon	*A. varicornis*		*C. purpureipennis*	
		Count	RSCU	Count	RSCU			Count	RSCU	Count	RSCU
Val	GUU(V)	71	1.49	64	1.42	Glu	GAA(E)	69	1.59	73	1.68
	GUC(V)	9	0.19	3	0.07		GAG(E)	18	0.41	14	0.32
	GUA(V)	89	1.87	95	2.11	Cys	UGU(C)	39	1.56	39	1.56
	GUG(V)	21	0.44	18	0.4		UGC(C)	11	0.44	11	0.44
Ser	UCU(S)	110	2.4	113	2.44	Trp	UGA(W)	85	1.77	86	1.74
	UCC(S)	20	0.44	28	0.6		UGG(W)	11	0.23	13	0.26
	UCA(S)	86	1.87	77	1.66	Arg	CGU(R)	17	1.24	19	1.41
	UCG(S)	7	0.15	8	0.17		CGC(R)	3	0.22	2	0.15
Pro	CCU(P)	80	2.39	68	2.09		CGA(R)	34	2.47	29	2.15
	CCC(P)	18	0.54	18	0.55		CGG(R)	1	0.07	4	0.3
	CCA(P)	35	1.04	39	1.2	Ser	AGU(S)	44	0.96	37	0.8
	CCG(P)	1	0.03	5	0.15		AGC(S)	14	0.31	11	0.24
Thr	ACU(T)	70	1.65	66	1.53		AGA(S)	84	1.83	97	2.09
	ACC(T)	24	0.56	22	0.51		AGG(S)	2	0.04	0	0
	ACA(T)	71	1.67	84	1.94	Gly	GGU(G)	52	1.02	62	1.2
	ACG(T)	5	0.12	1	0.02		GGC(G)	11	0.22	14	0.27
Ala	GCU(A)	63	1.81	48	1.34		GGA(G)	96	1.89	89	1.73
	GCC(A)	22	0.63	25	0.7		GGG(G)	44	0.87	41	0.8
	GCA(A)	51	1.47	66	1.85						
	GCG(A)	3	0.09	4	0.11						

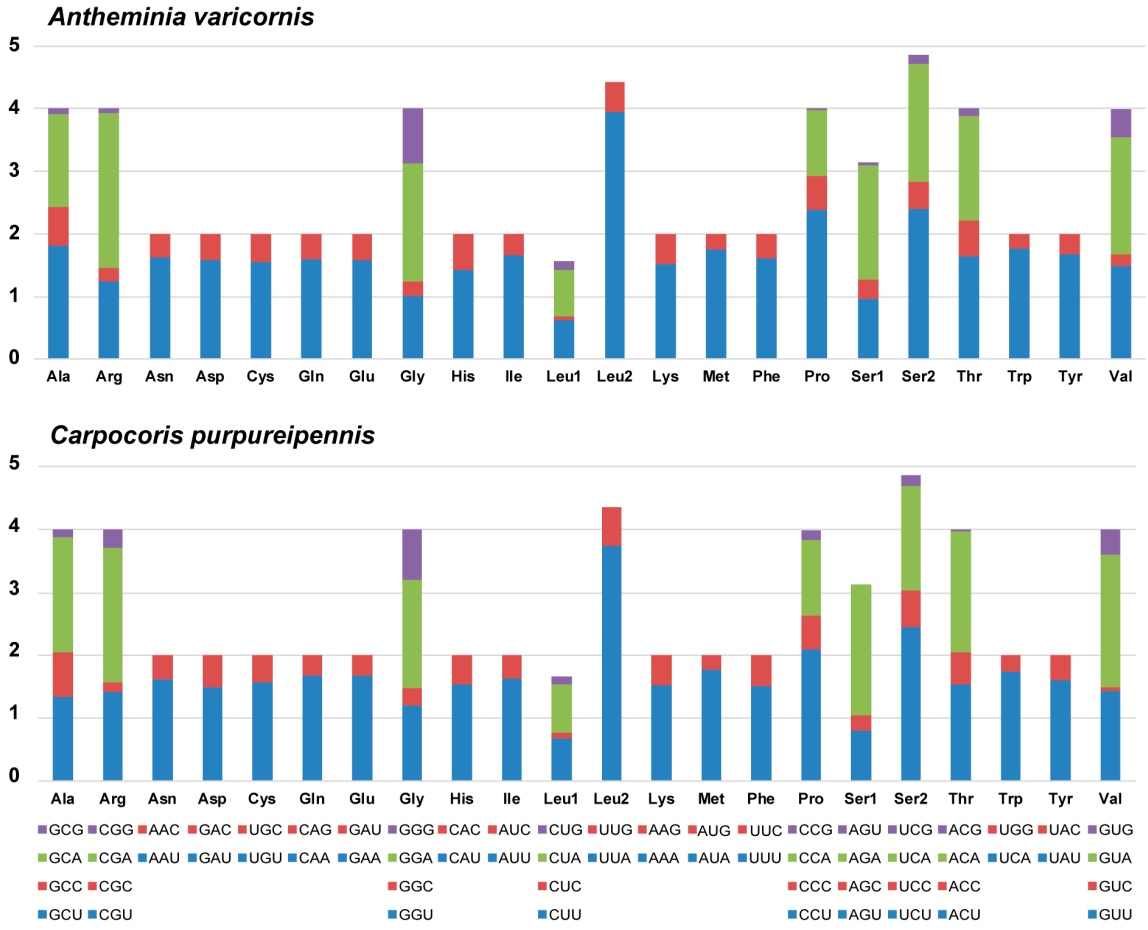

Figure 3. The relative synonymous codon usage (RSCU) in the mitogenomes of *A. varicornis* and *C. purpureipennis*. The *X*-axis shows the codons, and the *Y*-axis shows RSCU values. The upper and lower color interpretation is shared.

3.3. tRNAs, rRNAs and Control Region

Typical sets of 22 tRNA genes ranging in length from 62 to 72 bp have been identified in the mitogenomes of *A. varicornis* and *C. purpureipennis* (Tables 3 and 4), with variations in length. The A + T content of the concatenated tRNA genes is 75.7% and 73.9% for *A. varicornis* and *C. purpureipennis*, respectively. The nucleotide skews in the tRNA genes in the mitogenomes of the two species are consistent, with the concatenated tRNA genes exhibiting a positive AT-skew and a negative GC-skew (Table 5). Most tRNA genes can be folded into the typical cloverleaf secondary structure, while the dihydrouridine (DHU) arms of trnS (GCU) and trnV are very short, with only a single base pair. The non-Watson–Crick base pair G-U is common in tRNA genes from both species (Figures 4 and 5). The size of *A. varicornis* ranged from 62 bp (tRNA-Cys) to 71 bp (tRNA-Asp) while the size of *C. purpureipennis* ranged from 63 bp (tRNA-Ala) to 72 bp (tRNA-Lys). The total length of the 22 tRNAs of *A. varicornis* were 1472 bp, and the total length of the 22 tRNAs of *C. purpureipennis* were 1463 bp, respectively. Both 12S and 16S rRNA genes exhibit similar positions and sizes in the mitogenomes of *A. varicornis* and *C. purpureipennis* (Tables 3 and 4). The 12S rRNA exhibits a positive AT-skew and a negative GC-skew in both species. The 16S rRNA exhibits a negative AT-skew and a positive GC-skew in *A. varicornis* and a positive AT-skew and a negative GC-skew in *C. purpureipennis* (Table 5). The control regions of *A. varicornis* and *C. purpureipennis* are 595 and 682 bp in size (Tables 3 and 4), with A + T contents of 70.4% and 70.5%, respectively (Table 5).

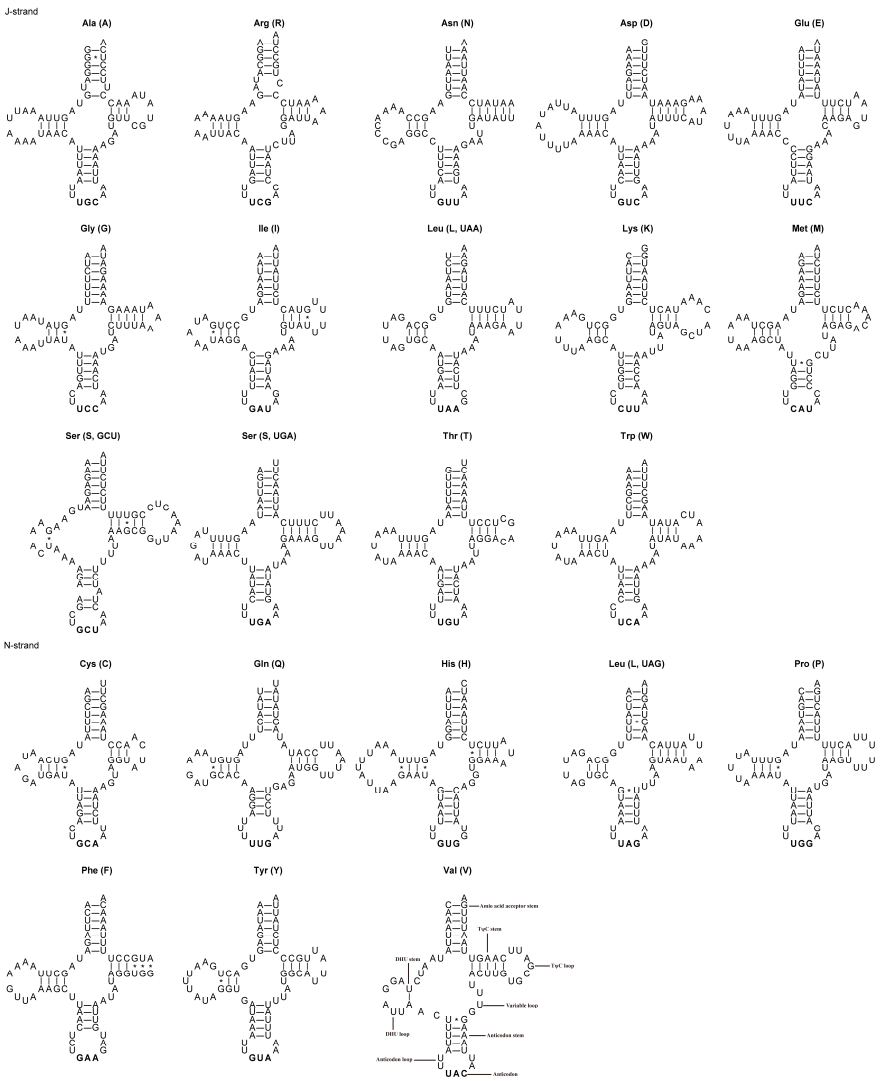

Figure 4. Secondary structure of 22 tRNAs in *A. varicornis*. * represents a non-classical pairing of G=U.

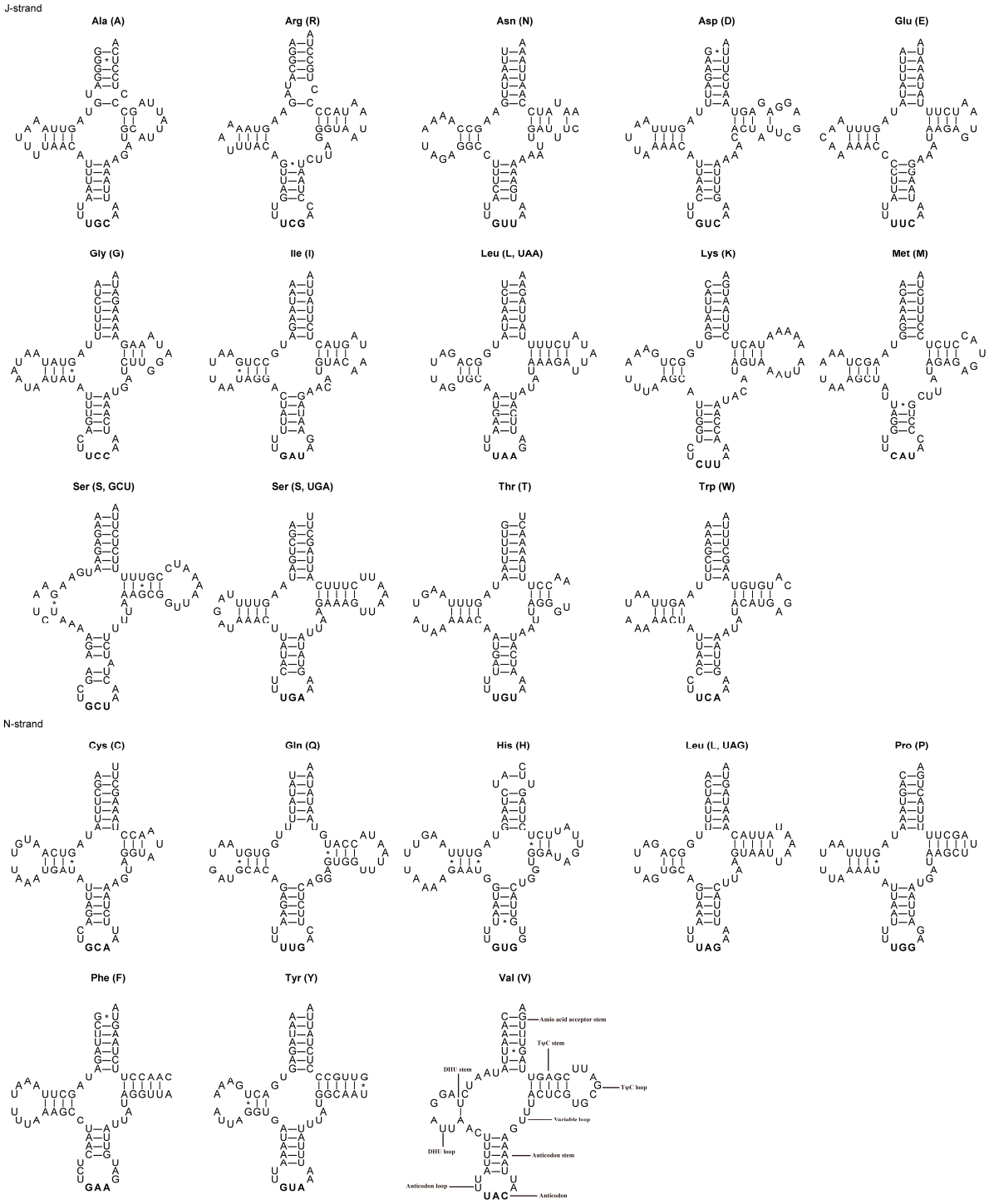

Figure 5. Secondary structure of 22 tRNAs in *C. purpureipennis*. * represents a non-classical pairing of G=U.

3.4. Phylogenetic Relationships

A previous study, based on small molecular fragments (1759 bp of 18S rRNA, 646 bp of 28S rRNA, 592 bp of 16S rRNA and 564 bp of COI), revealed that the *Antheminia* genus forms a sister group with *Carpocoris*, but there is low node support [38]. In this study, we selected one species from each genus as a representative taxon, used mitogenome data to verify this sister relationship, and further explored their phylogenetic positions within the Pentatomidae family. Phylogenetic analyses were performed using the BI and ML

methods based on the two datasets (PCG123R and PCG12R). All four phylogenetic trees show that *A. varicornis* forms a sister relationship with *C. purpureipennis* with high nodal support values (PP = 1 in BI trees; BS values = 100 in ML trees), which is consistent with the traditional taxonomy and the findings of a previous study [38].

In addition, all of the phylogenetic results support the fact that the two species form a sister group with *Dolycoris baccarum*, and then the three species together form a sister group with *Rubiconia intermedia* (Figures 6 and 7). This result is consistent with previous results based on molecular and morphological evidence; accordingly, we support the previous proposal that the species in the Eysarcorini and Carpocorini are closely related [37]. *Neojurtina typica* is in the most basic position within Pentatomidae. The phylogenetic tree constructed through ML and BI analysis showed a strong support for the monophyly of Asopinae and Phyllocephalinae, while the monophyly of Pentatominae and Podopinae was rejected (Figures 6 and 7).

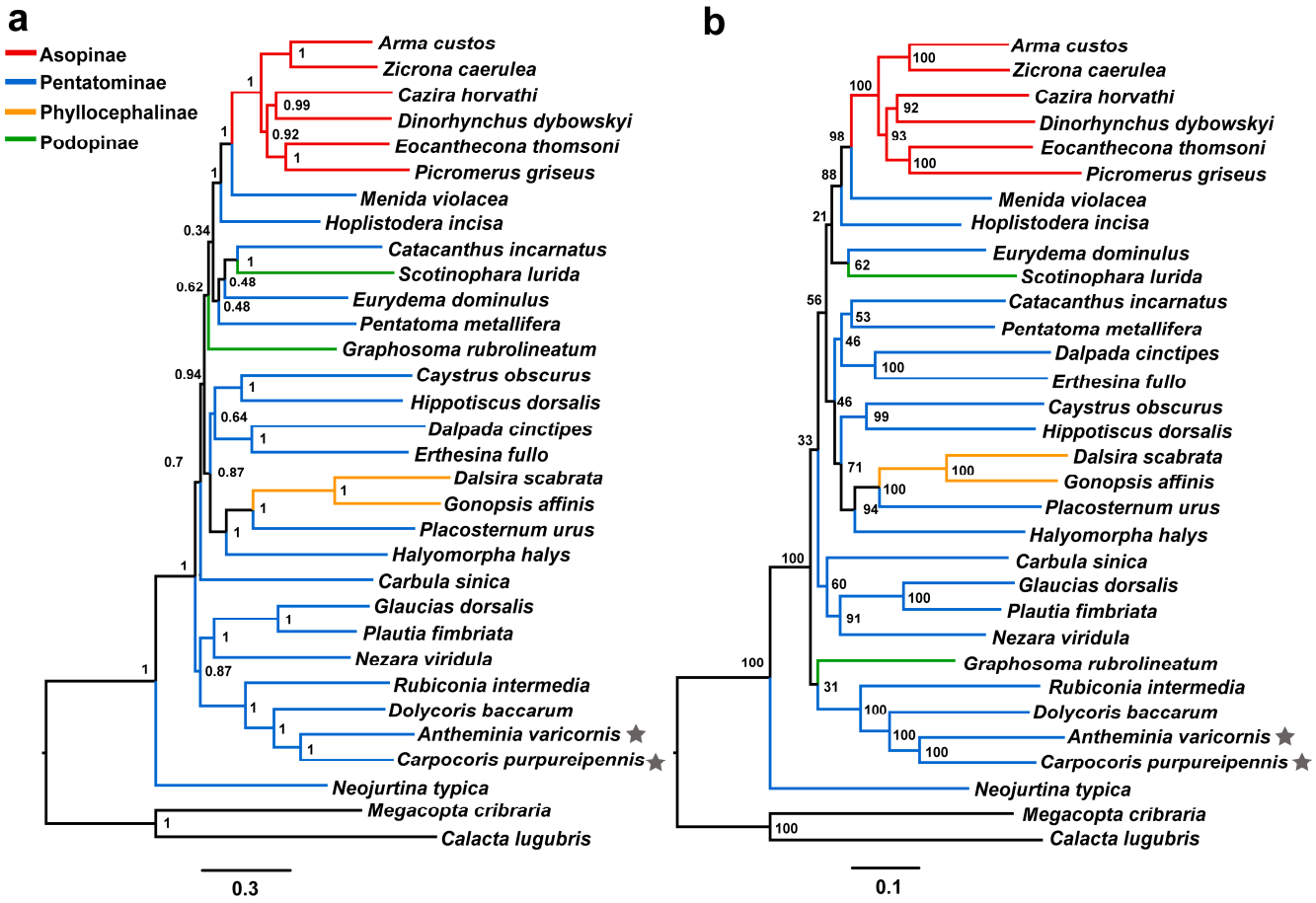

Figure 6. Phylogenetic relationships of Pentatomidae based on dataset PCG123R. Pentagram, the mt genome sequences of *A. varicornis* and *C. purpureipennis* in this study. The black lines are the two outgroups used in this study. (**a**) BI tree, numbers at the nodes are posterior probabilities; (**b**) ML tree, numbers at the nodes are bootstrap values.

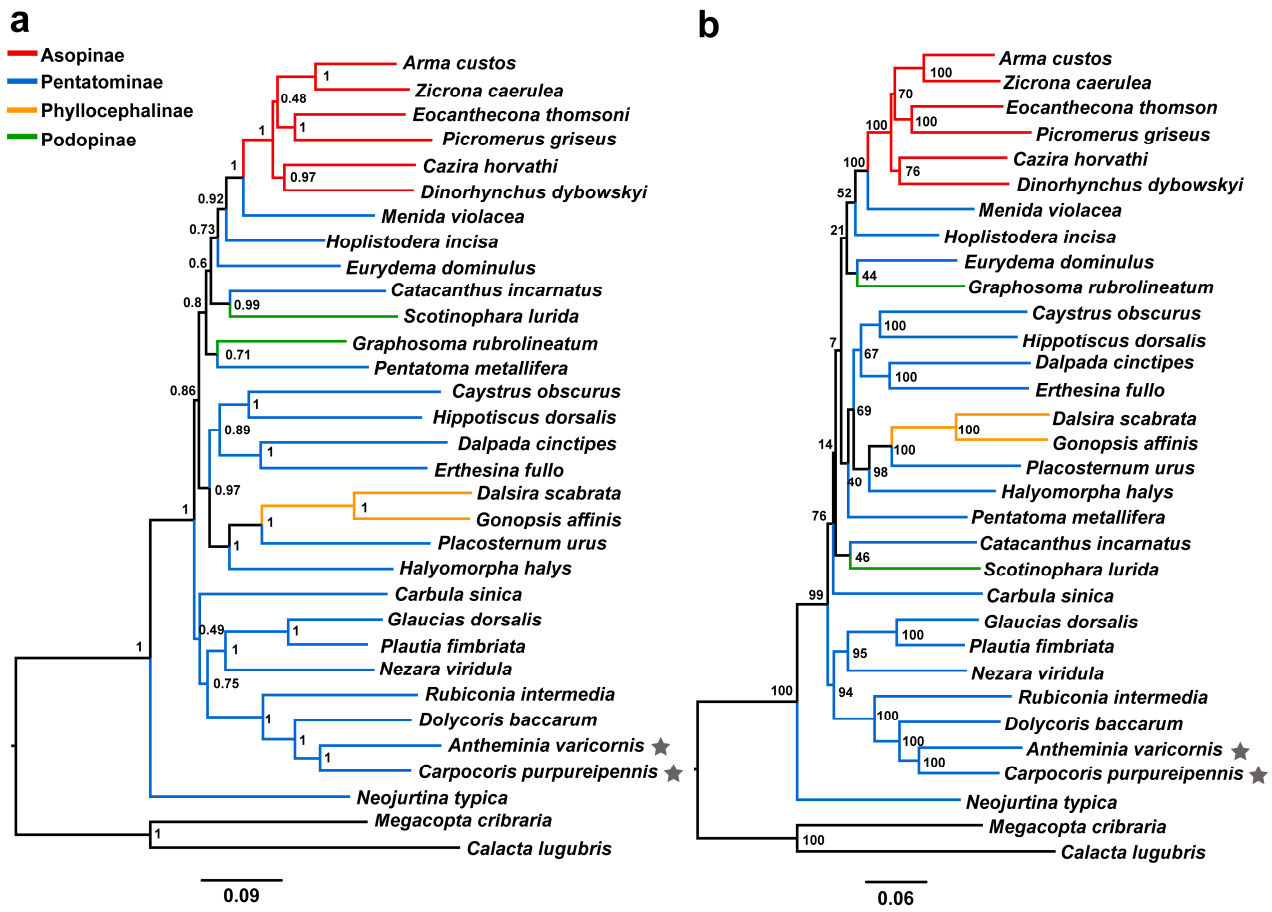

Figure 7. Phylogenetic relationships of Pentatomidae based on dataset PCG12R. Pentagram, the mt genome sequences of *A. varicornis* and *C. purpureipennis* in this study. The black lines are the two outgroups used in this study. (**a**) BI tree, numbers at the nodes are posterior probabilities; (**b**) ML tree, numbers at the nodes are bootstrap values.

4. Conclusions

In previous studies, more attention has been paid to the phylogenetic relationships of the higher order members of Heteroptera, while less attention has been paid to the phylogenetic relationships within the subfamily. In this study, two mitochondrial genomes from Pentatominae were sequenced and added to the existing data; we sequenced and analyzed the mitogenomes of *A. varicornis* and *C. purpureipennis*. The two mitogenomes are conserved in genomic structure, base composition, codon usage, and tRNA secondary structure.

We performed a phylogenetic analysis based on the sequences of thirteen PCGs and two rRNA genes. Our results strongly support the sister relationship between *A. varicornis* and *C. purpureipennis*. Our results provide a valuable resource for further phylogenetic and evolutionary analyses of the Pentatomidae, which also reveal the relationships among four subfamilies within Pentatomidae. The phylogenetic trees show a strong support for the monophyly of Asopinae and Phyllocephalinae, while the monophyly of Pentatominae and Podopinae was rejected. More mitochondrial genomes and nuclear genes need to be sequenced to reveal the mitochondrial genome evolution and phylogenetic relationships of Pentatominae more comprehensively.

Author Contributions: Y.W., C.Z. and W.B. conceived and designed the research. Y.W. and R.Y. conducted experiments. Y.W., R.Y. and X.Z. analyzed data. Y.W., C.Z. and W.B. wrote the manuscript. All authors have read and agreed to the published version of the manuscript.

Funding: This work was funded by the National Natural Science Foundation of China (31820103013, 32130014).

Institutional Review Board Statement: Not applicable.

Data Availability Statement: The data that support the findings of this study are openly available in GenBank (accession numbers: OR074478 and OR074479) at https://www.ncbi.nlm.nih.gov/ (accessed on 1 June 2023).

Conflicts of Interest: The authors declare no conflict of interest.

References

1. Wolstenholme, D.R. Animal mitochondrial DNA: Structure and evolution. *Int. Rev. Cytol.* **1992**, *141*, 173–216. [PubMed]
2. Boore, J.L. Animal mitochondrial genomes. *Nucleic Acids Res.* **1999**, *27*, 1767–1780. [CrossRef] [PubMed]
3. Cameron, S.L. Insect mitochondrial genomics: Implications for evolution and phylogeny. *Annu. Rev. Entomol.* **2014**, *59*, 95–117. [CrossRef] [PubMed]
4. Brown, W.M.; George, M.; Wilson, A.C. Rapid evolution of animal mitochondrial DNA. *Proc. Natl. Acad. Sci. USA* **1979**, *76*, 1967–1971. [CrossRef]
5. Curole, J.P.; Kocher, T.D. Mitogenomics: Digging deeper with complete mitochondrial genomes. *Trends Ecol. Evol.* **1999**, *14*, 394–398. [CrossRef]
6. Song, F.; Li, H.; Liu, G.H.; Wang, W.; James, P.; Colwell, D.D.; Tran, A.; Gong, S.; Cai, W.; Shao, R. Mitochondrial Genome Fragmentation Unites the Parasitic Lice of Eutherian Mammals. *Syst. Biol.* **2019**, *68*, 430–440. [CrossRef]
7. Du, Z.; Hasegawa, H.; Cooley, J.R.; Simon, C.; Yoshimura, J.; Cai, W.; Sota, T.; Li, H. Mitochondrial Genomics Reveals Shared Phylogeographic Patterns and Demographic History among Three Periodical Cicada Species Groups. *Mol. Biol. Evol.* **2019**, *36*, 1187–1200. [CrossRef]
8. Camacho, M.A.; Cadar, D.; Horváth, B.; Merino-Viteri, A.; Murienne, J. Revised phylogeny from complete mitochondrial genomes of phyllostomid bats resolves subfamilial classification. *Zool. J. Linn. Soc.* **2022**, *196*, 1591–1607. [CrossRef]
9. Ge, X.; Peng, L.; Vogler, A.P.; Morse, J.C.; Yang, L.; Sun, C.; Wang, B. Massive gene rearrangements of mitochondrial genomes and implications for the phylogeny of Trichoptera (Insecta). *Syst. Entomol.* **2022**, *48*, 278–295. [CrossRef]
10. Nielsen, M.; Margaryan, A.; Nielsen, T.L.; Enghoff, H.; Allentoft, M.E. Complete mitochondrial genomes from museum specimens clarify millipede evolution in the Eastern Arc Mountains. *Zool. J. Linn. Soc.* **2022**, *196*, 924–939. [CrossRef]
11. Kunde, M.N.; Barlow, A.; Klittich, A.M.; Yakupova, A.; Patel, R.P.; Fickel, J.; Forster, D.W. First mitogenome phylogeny of the sun bear *Helarctos malayanus* reveals a deep split between Indochinese and Sundaic lineages. *Ecol. Evol.* **2023**, *13*, e9969. [CrossRef] [PubMed]
12. Xing, Z.P.; Liang, X.; Wang, X.; Hu, H.Y.; Huang, Y.X. Novel gene rearrangement pattern in mitochondrial genome of *Ooencyrtusplautus* Huang & Noyes, 1994: New gene order in Encyrtidae (Hymenoptera, Chalcidoidea). *Zookeys* **2022**, *1124*, 1–21. [PubMed]
13. Pakrashi, A.; Patidar, A.; Singha, D.; Kumar, V.; Tyagi, K. Comparative analysis of the two suborders of Thysanoptera and characterization of the complete mitochondrial genome of *Thrips parvispinus*. *Arch. Insect Biochem. Physiol.* **2023**, *114*, e22010. [CrossRef] [PubMed]
14. Wu, Y.-Z.; Rédei, D.; Eger, J., Jr.; Wang, Y.-H.; Wu, H.-Y.; Carapezza, A.; Kment, P.; Cai, B.; Sun, X.-Y.; Guo, P.-L.; et al. Phylogeny and the colourful history of jewel bugs (Insecta: Hemiptera: Scutelleridae). *Cladistics* **2017**, *34*, 502–516. [CrossRef] [PubMed]
15. Zhang, D.L.; Li, M.; Li, T.; Yuan, J.J.; Bu, W.J. A mitochondrial genome of Micronectidae and implications for its phylogenetic position. *Int. J. Biol. Macromol.* **2018**, *119*, 747–757. [CrossRef]
16. Dong, X.; Wang, K.; Tang, Z.; Zhang, Y.; Yi, W.; Xue, H.; Zheng, C.; Bu, W. Phylogeny of Coreoidea based on mitochondrial genomes show the paraphyly of Coreidae and Alydidae. *Arch. Insect Biochem. Physiol.* **2022**, *110*, e21878. [CrossRef]
17. Liu, X.; He, J.; Du, Z.; Zhang, R.; Cai, W.; Li, H. Weak genetic structure of flower thrips *Frankliniella intonsa* in China revealed by mitochondrial genomes. *Int. J. Biol. Macromol.* **2023**, *231*, 123301. [CrossRef]
18. Li, H.; Leavengood, J.M.; Chapman, E.G., Jr.; Burkhardt, D.; Song, F.; Jiang, P.; Liu, J.; Zhou, X.; Cai, W. Mitochondrial phylogenomics of Hemiptera reveals adaptive innovations driving the diversification of true bugs. *Proc. R. Soc. B Biol. Sci.* **2017**, *284*, 20171223. [CrossRef]
19. Yang, H.; Li, T.; Dang, K.; Bu, W. Compositional and mutational rate heterogeneity in mitochondrial genomes and its effect on the phylogenetic inferences of Cimicomorpha (Hemiptera: Heteroptera). *BMC Genom.* **2018**, *19*, 264. [CrossRef]
20. Liu, Y.; Li, H.; Song, F.; Zhao, Y.; Wilson, J.J.; Cai, W. Higher-level phylogeny and evolutionary history of Pentatomomorpha (Hemiptera: Heteroptera) inferred from mitochondrial genome sequences. *Syst. Entomol.* **2019**, *44*, 810–819. [CrossRef]
21. Zheng, C.; Ye, Z.; Zhu, X.; Zhang, H.; Dong, X.; Chen, P.; Bu, W. Integrative taxonomy uncovers hidden species diversity in the rheophilic genus *Potamometra* (Hemiptera: Gerridae). *Zool. Scr.* **2019**, *49*, 174–186. [CrossRef]
22. Xu, S.; Wu, Y.; Liu, Y.; Zhao, P.; Chen, Z.; Song, F.; Li, H.; Cai, W. Comparative Mitogenomics and Phylogenetic Analyses of Pentatomoidea (Hemiptera: Heteroptera). *Genes* **2021**, *12*, 1306. [CrossRef] [PubMed]

23. Zhu, X.; Zheng, C.; Dong, X.; Zhang, H.; Ye, Z.; Xue, H.; Bu, W. Species boundary and phylogeographical pattern provide new insights into the management efforts of *Megacopta cribraria* (Hemiptera: Plataspidae), a bean bug invading North America. *Pest Manag. Sci.* **2022**, *78*, 4871–4881. [CrossRef] [PubMed]
24. Francoso, E.; Zuntini, A.R.; Ricardo, P.C.; Araujo, N.D.; Silva, J.P.N.; Brown, M.J.F.; Arias, M.C. The complete mitochondrial genome of *Trigonisca nataliae* (Hymenoptera, Apidae) assemblage reveals heteroplasmy in the control region. *Gene* **2023**, *881*, 147621. [CrossRef] [PubMed]
25. Zhou, S.X.; Wei, N.; Jost, M.; Wanke, S.; Rees, M.; Liu, Y.; Zhou, R.C. The Mitochondrial Genome of the Holoparasitic Plant *Thonningia sanguinea* Provides Insights into the Evolution of the Multichromosomal Structure. *Genome Biol. Evol.* **2023**, *15*, e155. [CrossRef] [PubMed]
26. Ke, S.J.; Liu, D.K.; Tu, X.D.; He, X.; Zhang, M.M.; Zhu, M.J.; Zhang, D.Y.; Zhang, C.L.; Lan, S.R.; Liu, Z.J. *Apostasia* Mitochondrial Genome Analysis and Monocot Mitochondria Phylogenomics. *Int. J. Mol. Sci.* **2023**, *24*, 7837. [CrossRef]
27. Kim, Y.K.; Jo, S.; Cheon, S.H.; Hong, J.R.; Kim, K.J. Ancient Horizontal Gene Transfers from Plastome to Mitogenome of a Nonphotosynthetic Orchid, *Gastrodia pubilabiata* (Epidendroideae, Orchidaceae). *Int. J. Mol. Sci.* **2023**, *24*, 11448. [CrossRef] [PubMed]
28. Xia, C.Y.; Li, J.L.; Zuo, Y.W.; He, P.; Zhang, H.; Zhang, X.X.; Wang, B.R.; Zhang, J.B.; Yu, J.; Deng, H.P. Complete mitochondrial genome of *Thuja sutchuenensis* and its implications on evolutionary analysis of complex mitogenome architecture in Cupressaceae. *BMC Plant Biol.* **2023**, *23*, 84. [CrossRef]
29. Wang, Y.; Chen, S.J.; Chen, J.J.; Chen, C.J.; Lin, X.J.; Peng, H.; Zhao, Q.; Wang, X.Y. Characterization and phylogenetic analysis of the complete mitochondrial genome sequence of *Photinia serratifolia*. *Sci. Rep.* **2023**, *13*, 770. [CrossRef]
30. Rider, D.; Schwertner, C.; Vilimova, J.; Redei, D.; Kment, P.; Thomas, D. *Higher Systematics of the Pentatomoidea*; CRC Press: Boca Raton, FL, USA, 2018.
31. Cesari, M.; Maistrello, L.; Ganzerli, F.; Dioli, P.; Rebecchi, L.; Guidetti, R. A pest alien invasion in progress: Potential pathways of origin of the brown marmorated stink bug *Halyomorpha halys* populations in Italy. *J. Pest Sci.* **2014**, *88*, 1–7. [CrossRef]
32. Mi, Q.; Zhang, J.; Gould, E.; Chen, J.; Sun, Z.; Zhang, F. Biology, Ecology, and Management of *Erthesina fullo* (Hemiptera: Pentatomidae): A Review. *Insects* **2020**, *11*, 346. [CrossRef] [PubMed]
33. Hua, J.; Li, M.; Dong, P.; Cui, Y.; Xie, Q.; Bu, W. Comparative and phylogenomic studies on the mitochondrial genomes of Pentatomomorpha (Insecta: Hemiptera: Heteroptera). *BMC Genom.* **2008**, *9*, 610. [CrossRef] [PubMed]
34. Zhang, Q.L.; Yuan, M.L.; Shen, Y.Y. The complete mitochondrial genome of *Dolycoris baccarum* (Insecta: Hemiptera: Pentatomidae). *Mitochondrial DNA* **2013**, *24*, 469–471. [CrossRef] [PubMed]
35. Yuan, M.L.; Zhang, Q.L.; Guo, Z.L.; Wang, J.; Shen, Y.Y. Comparative mitogenomic analysis of the superfamily Pentatomoidea (Insecta: Hemiptera: Heteroptera) and phylogenetic implications. *BMC Genom.* **2015**, *16*, 460. [CrossRef] [PubMed]
36. Zhao, L.; Wei, J.; Zhao, W.; Chen, C.; Gao, X.; Zhao, Q. The complete mitochondrial genome of *Pentatoma rufipes* (Hemiptera, Pentatomidae) and its phylogenetic implications. *Zookeys* **2021**, *1042*, 51–72. [CrossRef] [PubMed]
37. Lian, D.; Wei, J.; Chen, C.; Niu, M.; Zhang, H.; Zhao, Q. Comparative analysis and phylogeny of mitochondrial genomes of Pentatomidae (Hemiptera: Pentatomoidea). *Front. Genet.* **2022**, *13*, 1045193. [CrossRef] [PubMed]
38. Roca-Cusachs, M.; Schwertner, C.F.; Kim, J.; Eger, J.; Grazia, J.; Jung, S. Opening Pandora's box: Molecular phylogeny of the stink bugs (Hemiptera: Heteroptera: Pentatomidae) reveals great incongruences in the current classification. *Syst. Entomol.* **2021**, *47*, 36–51. [CrossRef]
39. Chen, S.; Zhou, Y.; Chen, Y.; Gu, J. fastp: An ultra-fast all-in-one FASTQ preprocessor. *Bioinformatics* **2018**, *34*, i884–i890. [CrossRef]
40. Meng, G.; Li, Y.; Yang, C.; Liu, S. MitoZ: A toolkit for animal mitochondrial genome assembly, annotation and visualization. *Nucleic Acids Res.* **2019**, *47*, e63. [CrossRef]
41. Peng, Y.; Leung, H.C.; Yiu, S.M.; Chin, F.Y. IDBA-UD: A de novo assembler for single-cell and metagenomic sequencing data with highly uneven depth. *Bioinformatics* **2012**, *28*, 1420–1428. [CrossRef]
42. Grant, J.R.; Enns, E.; Marinier, E.; Mandal, A.; Herman, E.K.; Chen, C.Y.; Graham, M.; Van Domselaar, G.; Stothard, P. Proksee: In-Depth characterization and visualization of bacterial genomes. *Nucleic Acids Res.* **2023**, *51*, W484–W492. [CrossRef]
43. Kumar, S.; Stecher, G.; Li, M.; Knyaz, C.; Tamura, K. MEGA X: Molecular Evolutionary Genetics Analysis across Computing Platforms. *Mol. Biol. Evol.* **2018**, *35*, 1547–1549. [CrossRef] [PubMed]
44. Katoh, K.; Standley, D.M. MAFFT Multiple Sequence Alignment Software Version 7: Improvements in Performance and Usability. *Mol. Biol. Evol.* **2013**, *30*, 772–780. [CrossRef] [PubMed]
45. Zhang, D.; Gao, F.; Jakovlić, I.; Zou, H.; Zhang, J.; Li, W.X.; Wang, G.T. PhyloSuite: An integrated and scalable desktop platform for streamlined molecular sequence data management and evolutionary phylogenetics studies. *Mol. Ecol. Resour.* **2019**, *20*, 348–355. [CrossRef] [PubMed]
46. Lanfear, R.; Frandsen, P.B.; Wright, A.M.; Senfeld, T.; Calcott, B. PartitionFinder 2: New Methods for Selecting Partitioned Models of Evolution for Molecular and Morphological Phylogenetic Analyses. *Mol. Biol. Evol.* **2017**, *34*, 772–773. [CrossRef] [PubMed]
47. Ronquist, F.; Teslenko, M.; Van Der Mark, P.; Ayres, D.L.; Darling, A.; Hohna, S.; Larget, B.; Liu, L.; Suchard, M.A.; Huelsenbeck, J.P. MrBayes 3.2: Efficient Bayesian phylogenetic inference and model choice across a large model space. *Syst. Biol.* **2012**, *61*, 539–542. [CrossRef]
48. Nguyen, L.T.; Schmidt, H.A.; Von Haeseler, A.; Minh, B.Q. IQ-TREE: A fast and effective stochastic algorithm for estimating maximum-likelihood phylogenies. *Mol. Biol. Evol.* **2015**, *32*, 268–274. [CrossRef]

49. Clary, D.O.; Wolstenholme, D.R. The mitochondrial DNA molecule of *Drosophila yakuba*: Nucleotide sequence, gene organization, and genetic code. *J. Mol. Evol.* **1985**, *22*, 252–271. [CrossRef]
50. Hassanin, A.; Leger, N.; Deutsch, J. Evidence for multiple reversals of asymmetric mutational constraints during the evolution of the mitochondrial genome of Metazoa, and consequences for phylogenetic inferences. *Syst. Biol.* **2005**, *54*, 277–298. [CrossRef]
51. Ojala, D.; Montoya, J.; Attardi, G. tRNA punctuation model of RNA processing in human mitochondria. *Nature* **1981**, *290*, 470–474. [CrossRef]